

Finite Mixtures of Multivariate Poisson-Log Normal Factor Analyzers for Clustering Count Data

Andrea Payne^{*†} Anjali Silva^{*‡} Steven J. Rothstein[§]
 Paul D. McNicholas[¶] Sanjeena Subedi[†]

Abstract

A mixture of multivariate Poisson-log normal factor analyzers is introduced by imposing constraints on the covariance matrix, which resulted in flexible models for clustering purposes. In particular, a class of eight parsimonious mixture models based on the mixtures of factor analyzers model are introduced. Variational Gaussian approximation is used for parameter estimation, and information criteria are used for model selection. The proposed models are explored in the context of clustering discrete data arising from RNA sequencing studies. Using real and simulated data, the models are shown to give favourable clustering performance. The GitHub R package for this work is available at <https://github.com/anjalisilva/mixMPLNFA> and is released under the open-source MIT license.

1 Introduction

Model-based clustering is a technique that utilizes finite mixture models to cluster data (Wolfe, 1965; Hand, 1989; McLachlan and Peel, 2000; McNicholas, 2016). The general distribution function for mixture models can be given as

$$f(\mathbf{y}|\pi_1, \dots, \pi_G, \boldsymbol{\vartheta}_1, \dots, \boldsymbol{\vartheta}_G) = \sum_{g=1}^G \pi_g f_g(\mathbf{y}|\boldsymbol{\vartheta}_g),$$

where G is the total number of clusters, $f_g(\cdot)$ is the distribution function with parameters $\boldsymbol{\vartheta}_g$, and $\pi_g > 0$ is the mixing weight of the g^{th} component such that $\sum_{g=1}^G \pi_g = 1$. Mixture

^{*}Co-first authors

[†]School of Mathematics and Statistics, Carleton University, Ottawa, ON, Canada.

[‡]Princess Margaret Cancer Centre - University Health Network, Toronto, ON, Canada; University of Toronto Libraries, Toronto, ON, Canada.

[§]Department of Molecular and Cellular Biology, University of Guelph, Guelph, ON, Canada.

[¶]Department of Mathematics and Statistics, McMaster University, Hamilton, ON, Canada.

model-based clustering methods can be over-parameterized in high-dimensional spaces, especially as the number of clusters increases. Subspace clustering allows for clustering data in low-dimensional subspaces while utilizing information from all the dimensions and by introducing restrictions to mixture parameters (Bouveyron and Brunet, 2012). Restrictions are introduced to the model parameters to obtain parsimonious models, which provide various possible covariance structures while reducing the number of parameters to fit.

Clustering multivariate count data is of interest in a variety of fields, including, but not limited to, bioinformatics, text mining, and sports analytics (Subedi and Browne, 2020). Specifically within bioinformatics, this form of clustering has become increasingly popular as researchers aim to sort data into homogeneous subgroups so differing characteristics can be identified and analyzed (Subedi and Browne, 2020). Many novel clustering methods have been proposed in recent years; de Souto et al. (2008) compare these methods to more traditional clustering methods, finding that a mixture model-based clustering approach outperformed the rest in the context of clustering cancer tissues for subtype identification. In the years since this publication, further research has proposed advancements to this approach and new methods for mixture model clustering for variety of data types (Bouveyron and Brunet, 2012; Gollini and Murphy, 2014; Subedi and McNicholas, 2014; Vrbik and McNicholas, 2014; Subedi et al., 2015; Browne and McNicholas, 2015; Dang et al., 2015; Kosmidis and Karlis, 2016; Tortora et al., 2019; Subedi and McNicholas, 2020; Subedi and Browne, 2020). These proposed methods focus on a variety of distributions and methods of parameter estimation.

RNA sequencing (RNA-seq) is a specific area of interest within the field of bioinformatics for applications of model-based clustering. RNA-seq is used to determine the transcriptional dynamics of a biological system by measuring the expression levels of many genes (Wang et al., 2009; Roberts et al., 2011). This technique provides counts of reads that can be mapped back to a biological entity. Di et al. (2011) note that negative binomial-based models can account for variability in RNA-seq data while also requiring less statistical power. As such, negative binomial models have been utilized to cluster RNA-seq data as well (Si et al., 2014). However, as stated by Silva et al. (2019), clustering methods based on a univariate distribution such as negative binomial distribution can struggle with clustering multivariate RNA-seq data as such models assume independence between variables. Hence, in this paper, we will develop a method based on multivariate Poisson-log normal distributions (Aitchison and Ho, 1989; Silva et al., 2019) which can account for overdispersion and also accommodate positive and negative correlations.

The factor analysis model by Spearman (1904) assumes that a d -dimensional vector of observed variables, \mathbf{X} , can be modelled by a K -dimensional vector of latent factors, where $K < d$. As a result, the factor analysis model is useful in modelling the covariance structure of high-dimensional data using a small number of latent variables. The mixture of factor analyzers model was later introduced by Ghahramani et al. (1996) and this model can perform clustering and local dimensionality reduction within each cluster concurrently. Consider n independent d -dimensional continuous variables $\mathbf{X}_1, \dots, \mathbf{X}_n$, which come from a heterogeneous population with G subgroups. In the mixture of factor analyzers framework,

\mathbf{X}_i is modelled as

$$\mathbf{X}_i = \boldsymbol{\mu}_g + \boldsymbol{\Lambda}_g \mathbf{U}_{ig} + \boldsymbol{\epsilon}_{ig} \text{ with probability } \pi_g,$$

for $i = 1, \dots, n$ and $g = 1, \dots, G$. Here, $\boldsymbol{\mu}_g$ is a $d \times 1$ vector of g th component mean, $\boldsymbol{\Lambda}_g$ is a $d \times K$ matrix of g th component factor loadings, $\mathbf{U}_{ig} \sim \mathcal{N}_K(\mathbf{0}, \mathbf{I}_K)$ is a $K \times 1$ vector of g th component latent factors, and $\boldsymbol{\epsilon}_{ig} \sim \mathcal{N}_d(\mathbf{0}, \boldsymbol{\Psi}_g)$ is a $d \times 1$ vector of g th component errors with $\boldsymbol{\Psi}_g = \text{diag}(\psi_{g1}, \dots, \psi_{gd})$. Note that the \mathbf{U}_{ig} are independently distributed and are independent of the $\boldsymbol{\epsilon}_{ig}$, which are also independently distributed. Under this model, the density of \mathbf{X}_i from a mixture of factor analyzer models is

$$f(\mathbf{x}_i | \boldsymbol{\Theta}) = \sum_{g=1}^G \pi_g f_g(\mathbf{x}_i | \boldsymbol{\mu}_g, \boldsymbol{\Lambda}_g \boldsymbol{\Lambda}_g' + \boldsymbol{\Psi}_g),$$

where, $\boldsymbol{\Theta} = (\pi_1, \dots, \pi_G, \boldsymbol{\mu}_1, \dots, \boldsymbol{\mu}_G, \boldsymbol{\Lambda}_1, \dots, \boldsymbol{\Lambda}_G, \boldsymbol{\Psi}_1, \dots, \boldsymbol{\Psi}_G)$. Further, $\mathbf{X}_i | \mathbf{u}_{ig} \sim \mathcal{N}_d(\boldsymbol{\mu}_g + \boldsymbol{\Lambda}_g \mathbf{u}_{ig}, \boldsymbol{\Psi}_g)$. It should be noted that the $\boldsymbol{\Lambda}_g$ is not uniquely defined for $K > 1$. Therefore the K -dimensional space in which the factors lie can be determined, but the directions of these factors cannot be determined. However, this does not affect the clustering algorithm, because $\boldsymbol{\Lambda}_g \boldsymbol{\Lambda}_g'$ is unique. The number of free g^{th} component covariance parameters that are reduced using the factor analysis model is

$$\frac{1}{2}d(d+1) - \left[dK + d - \frac{1}{2}K(K-1) \right] = \frac{1}{2} \left[(d-K)^2 - (d+K) \right],$$

given that $(d-K)^2 > (d+K)$ (Lawley and Maxwell, 1962; McNicholas, 2016).

In 2008, this work was extended and a family of eight parsimonious Gaussian mixture models (PGMMs; McNicholas and Murphy, 2008) were introduced with parsimonious covariance structures. The PGMM family arises by considering the general mixture of factor analyzers model ($\boldsymbol{\Sigma}_g = \boldsymbol{\Lambda}_g \boldsymbol{\Lambda}_g' + \boldsymbol{\Psi}_g$) and by allowing the constraints $\boldsymbol{\Lambda}_g = \boldsymbol{\Lambda}$, $\boldsymbol{\Psi}_g = \boldsymbol{\Psi}$, and the isotropic constraint $\boldsymbol{\Psi}_g = \psi_g \mathbf{I}_d$. These covariance structures can have as few as $dK - K(K-1)/2 + 1$ free parameters or as many as $G[dK - K(K-1)/2 + d]$ free parameters. With the introduction of the factor analysis structure, the number of covariance parameters is linear in data dimensionality, thus making this family well suited for analysis of high-dimensional data (McNicholas and Murphy, 2010). The constraints allow for assuming a common structure in the component covariance matrix $\boldsymbol{\Sigma}_g$ between clusters, if appropriate, and this enables a parsimonious model.

Previously, a model-based clustering methodology using a mixture of multivariate Poisson-log normal distributions (MPLN; Aitchison and Ho, 1989) was developed to analyze multivariate count measurements from RNA-seq studies (Silva et al., 2019). A d -dimensional random variable following a G -component mixtures of MPLN distribution is said to have a total of $G - 1 + Gd + Gd(d+1)/2$ free parameters. Here, $G - 1$ parameters are contributed by the mixing proportions, Gd from the means and $Gd(d+1)/2$ from the covariance matrices. Since the largest contribution is through the covariance matrices, it is a natural focus for the introduction of parsimony.

In this work, a family of mixtures of MPLN factor analyzers that is analogous to the PGMM family is developed, by considering the constraints $\Lambda_g = \Lambda$ and $\Psi_g = \Psi$. This family is referred to as the parsimonious mixtures of the MPLN factor analyzers family (MPLNFA). The proposed model simultaneously performs factor analysis and cluster analysis, by assuming that the discrete observed data have been generated by a factor analyzer model in the continuous latent variables. Details of parameter estimation are provided, and both real and simulated data illustrations are used to demonstrate the clustering ability.

2 Methodology

2.1 Mixtures of Factor Analyzer

Suppose \mathbf{Y}_{ij} denotes the observed counts of the i^{th} sample for the j^{th} variable and \mathbf{X}_{ij} denotes the associated underlying latent variable. To develop a mixture of factor analyzers, we assume the following hierarchical structure with the K -dimensional latent factor \mathbf{U}_i :

$$\begin{aligned} Y_{ij} \mid X_{ij} = x_{ij} &\sim \text{Poisson}(\exp\{x_{ij} + \log C_i\}), \\ \mathbf{X}_i \mid \mathbf{U}_i = \mathbf{u}_i &\sim N(\boldsymbol{\mu}_g + \Lambda_g \mathbf{u}_i, \Psi_g), \\ \mathbf{U}_i &\sim N(\mathbf{0}_K, \mathbf{I}_K). \end{aligned}$$

Here, C_i is a fixed known constant representing the normalized library sizes added to account for the differences in the library sizes of the i^{th} sample.

In model-based clustering, we also have unobserved component membership indicator variable \mathbf{Z} such that $Z_{ig} = 1$ if the observation i^{th} belongs to group g and $Z_{ig} = 0$ otherwise. Hence, the complete data now comprises observed expression levels \mathbf{y} , underlying latent variable \mathbf{X} , and unknown group membership \mathbf{Z} . The complete-data likelihood can therefore be written as:

$$L(\boldsymbol{\vartheta}) = \prod_{g=1}^G \prod_{i=1}^n \left[\pi_g \left\{ \prod_{j=1}^d f(y_{ij} \mid x_{ij}, C_i) \right\} f(\mathbf{x}_i \mid \mathbf{u}_i, \boldsymbol{\mu}_g, \Lambda_g, \Psi_g) f(\mathbf{u}_i) \right]^{z_{ig}},$$

where $\boldsymbol{\vartheta}$ denotes all the model parameters. The complete data log-likelihood can therefore be written as:

$$l_c(\boldsymbol{\vartheta}) = \sum_{g=1}^G \sum_{i=1}^n z_{ig} \left[\log \pi_g + \left\{ \sum_{j=1}^d \log f(y_{ij} \mid x_{ij}, k_j) \right\} + \log f(\mathbf{x}_i \mid \mathbf{u}_i, \boldsymbol{\mu}_g, \Lambda_g, \Psi_g) + \log f(\mathbf{u}_i) \right],$$

To utilize the expectation-maximization (EM) framework for parameter estimation, we require $\mathbb{E}(Z_{ig} \mathbf{X}_i \mid \mathbf{y}_i, \mathbf{u}_i, \boldsymbol{\mu}_g, \Lambda_g, \Psi_g)$, $\mathbb{E}(Z_{ig} \mathbf{X}_i \mathbf{X}_i' \mid \mathbf{y}_i, \mathbf{u}_i, \boldsymbol{\mu}_g, \Lambda_g, \Psi_g)$, $\mathbb{E}(Z_{ig} \mathbf{U}_i \mid \mathbf{y}_i, \mathbf{x}_i, \boldsymbol{\mu}_g, \Lambda_g, \Psi_g)$

and $\mathbb{E}(Z_{ig} \mathbf{U}_i \mathbf{U}_i' | \mathbf{y}_i, \mathbf{x}_i, \boldsymbol{\mu}_g, \boldsymbol{\Lambda}_g, \boldsymbol{\Psi}_g)$. To compute these quantities, we need the posterior distribution of $\mathbf{X}_i | \mathbf{y}_i, \mathbf{u}_i$ which does not have a closed form. Thus, parameter estimation relies on the Markov chain Monte Carlo expectation-maximization (MCMC-EM) approach which can be computationally intensive.

2.2 Variational approximation of mixtures of MPLN factor analyzers

Subedi and Browne (2020) proposed a framework for parameter estimation utilizing variational Gaussian approximation (VGA) for MPLN-based mixture models. Variational approximation (Wainwright et al., 2008) is an approximate inference technique that uses a computationally convenient approximating density in place of a more complex but ‘true’ posterior density obtained by minimizing the Kullback-Leibler (KL) divergence between the true and the approximating densities. Markov chain Monte Carlo expectation-maximization (MCMC-EM) has also been used for parameter estimation of MPLN-based mixture models, but VGA was shown to be computationally efficient (Silva et al., 2023). Here, we propose a mixture of Poisson log-normal distributions with factor analyzers that utilize a variational EM framework for parameter estimation.

Parameter estimation for a mixture of factor analyzers is typically done using an alternating expectation conditional maximization (AECM) framework that assumes different specifications of missing data at different stages. Here, we will adopt a similar notion resulting in a two-stage iterative EM-type approach.

2.3 Stage 1

In Stage 1, we treat \mathbf{X} and \mathbf{Z} as missing such that

$$\begin{aligned} Y_{ij} | X_{ij} = x_{ij} &\sim \text{Poisson}(\exp\{x_{ij} + \log C_i\}) \\ \mathbf{X}_i &\sim N(\boldsymbol{\mu}_g, \boldsymbol{\Sigma}_g), \end{aligned}$$

where $\boldsymbol{\Sigma}_g = \boldsymbol{\Lambda}_g \boldsymbol{\Lambda}_g^T + \boldsymbol{\Psi}_g$. Therefore, the component-specific marginal density of the observed data \mathbf{y}_i can be written as

$$f(\mathbf{y}_i | Z_{ig} = 1, \boldsymbol{\mu}_g, \boldsymbol{\Sigma}_g) = \int_{\mathbb{R}^d} \left[\prod_{j=1}^d f_p(y_{ij} | x_{ij}, C_i, Z_{ig} = 1) \right] f_N(\mathbf{x}_i | Z_{ig} = 1, \boldsymbol{\mu}_g, \boldsymbol{\Sigma}_g) d\mathbf{x}_i,$$

where x_{ij} and y_{ij} are the j^{th} element of \mathbf{x}_i and \mathbf{y}_i respectively, $f_p(\cdot)$ is the probability mass function of the Poisson distribution with mean $e^{x_{ij} + \log C_j}$ and $f_N(\cdot)$ is the probability density function of d -dimensional Gaussian distribution with mean $\boldsymbol{\mu}_g$ and covariance $\boldsymbol{\Sigma}_g$. Note that the marginal distribution of \mathbf{Y} involves multiple integrals and cannot be further simplified.

The complete-data log-likelihood using the marginal density of $\mathbf{y}_i \mid Z_{ig} = 1$ can be written as:

$$l(\boldsymbol{\vartheta}) = \sum_{g=1}^G \sum_{i=1}^n z_{ig} \log \pi_g + \sum_{g=1}^G \sum_{i=1}^n z_{ig} \log f(\mathbf{y}_i \mid Z_{ig} = 1, \boldsymbol{\mu}_g, \boldsymbol{\Sigma}_g).$$

As the marginal of $\mathbf{Y}_i \mid Z_{ig} = 1$ cannot be simplified, we use variational Gaussian approximation to approximate the marginal of \mathbf{Y}_i from component g in the mixtures of MPLN distributions. Suppose, we have an approximating density $q(\mathbf{x}_{ig})$, we can write

$$\log f(\mathbf{y}_i \mid Z_{ig} = 1) = F(q_{ig}, \mathbf{y}_i) + D_{KL}(q_{ig} \parallel f_{ig}),$$

where $D_{KL}(q_{ig} \parallel f_{ig}) = \int_{\mathbb{R}^d} q(\mathbf{x}_{ig}) \log \frac{q(\mathbf{x}_{ig})}{f(\mathbf{x}_i \mid \mathbf{y}_i, Z_{ig}=1)} d\mathbf{x}_{ig}$ is the Kullback-Leibler (KL) divergence between $f(\mathbf{x}_i \mid \mathbf{y}_i, Z_{ig} = 1)$ and approximating distribution $q(\mathbf{x}_{ig})$, and

$$F(q_{ig}, \mathbf{y}_i) = \int_{\mathbb{R}^d} [\log f(\mathbf{y}_i, \mathbf{x}_i \mid Z_{ig} = 1) - \log q(\mathbf{x}_{ig})] q(\mathbf{x}_{ig}) d\mathbf{x}_{ig},$$

is our evidence lower bound (ELBO) for each observation \mathbf{y}_i . Details can be found in Appendix A.1. The complete data log-likelihood of the mixtures of MPLN distributions can be written as:

$$l_c(\boldsymbol{\vartheta} \mid \mathbf{y}) = \sum_{g=1}^G \sum_{i=1}^n z_{ig} \log \pi_g + \sum_{g=1}^G \sum_{i=1}^n z_{ig} [F(q_{ig}, \mathbf{y}_i) + D_{KL}(q_{ig} \parallel f_{ig})].$$

In VGA, $q(\mathbf{x}_{ig})$ is assumed to be a Gaussian distribution. Assuming $q(\mathbf{x}_{ig}) = \mathcal{N}(\mathbf{m}_{ig}, \mathbf{S}_{ig})$, the ELBO for each observation \mathbf{y}_i becomes

$$\begin{aligned} F(q_{ig}, \mathbf{y}_i) = & \\ & - \frac{1}{2}(\mathbf{m}_{ig} - \boldsymbol{\mu}_g)' \boldsymbol{\Sigma}_g^{-1} (\mathbf{m}_{ig} - \boldsymbol{\mu}_g) - \frac{1}{2} \text{tr}(\boldsymbol{\Sigma}_g^{-1} \mathbf{S}_{ig}) + \frac{1}{2} \log |\mathbf{S}_{ig}| - \frac{1}{2} \log |\boldsymbol{\Sigma}_g| + \frac{d}{2} \\ & + \mathbf{m}'_{ig} \mathbf{y}_i + \sum_{j=1}^d (\log C_i) y_{ij} - \sum_{j=1}^d \left\{ e^{\log C_i + m_{igj} + \frac{1}{2} S_{ig,jj}} + \log(y_{ij}!) \right\}. \end{aligned}$$

Thus, to minimize the KL divergence between the true and approximating density, we find the values of the variational parameters \mathbf{m}_{ig} and \mathbf{S}_{ig} that maximize our ELBO. Similar to Arridge et al. (2018) and Subedi and Browne (2020), estimation of the mean (\mathbf{m}_{ig}) and variance (\mathbf{S}_{ig}) can be obtained via Newton's method and fixed-point method.

Therefore, in Stage 1, we update $\mathbb{E}(Z_{ig} \mid \mathbf{y}_i)$, variational parameters \mathbf{m}_{ig} and \mathbf{S}_{ig} , and model parameters π_g and $\boldsymbol{\mu}_g$.

1. Conditional on the variational parameters $\mathbf{m}_{ig}, \mathbf{S}_{ig}$ and on $\boldsymbol{\mu}_g$ and $\boldsymbol{\Sigma}_g$, the $\mathbb{E}(Z_{ig})$ is computed. Given $\boldsymbol{\mu}_g$ and $\boldsymbol{\Sigma}_g$,

$$\mathbb{E}(Z_{ig} \mid \mathbf{y}_i) = \frac{\pi_g f(\mathbf{y} \mid \boldsymbol{\mu}_g, \boldsymbol{\Sigma}_g)}{\sum_{h=1}^G \pi_h f(\mathbf{y} \mid \boldsymbol{\mu}_h, \boldsymbol{\Sigma}_h)}.$$

Note that this involves the marginal distribution of \mathbf{Y} which is difficult to compute. Hence, similar to Subedi and Browne (2020), we use an approximation of $\mathbb{E}(Z_{ig})$ where we replace the marginal density of the exponent of ELBO such that

$$\widehat{Z}_{ig} \stackrel{\text{def}}{=} \frac{\pi_g \exp [F(q_{ig}, \mathbf{y}_i)]}{\sum_{h=1}^G \pi_h \exp [F(q_{ih}, \mathbf{y}_i)]}.$$

2. Update the variational parameters \mathbf{m}_{ig} and \mathbf{S}_{ig} as following:

(a) Fixed-point method for updating \mathbf{S}_{ig} is

$$\mathbf{S}_{ig}^{(t+1)} = \left\{ \boldsymbol{\Sigma}_g^{-1} + \mathbf{I} \odot \mathbf{exp} \left[\log C_i + \mathbf{m}_{ig}^{(t)} + \frac{1}{2} \text{diag} \left(\mathbf{S}_{ig}^{(t)} \right) \right] \mathbf{1}'_d \right\}^{-1}$$

where the vector function $\mathbf{exp}[\mathbf{a}] = (e^{a_1}, \dots, e^{a_d})'$ is a vector of exponential each element of the d -dimensional vector \mathbf{a} , $\text{diag}(\mathbf{S}) = (\mathbf{S}_{11} \dots, \mathbf{S}_{dd})$ puts the diagonal elements of the $d \times d$ matrix \mathbf{S} into a d -dimensional vector, \odot the Hadmard product and $\mathbf{1}_d$ is a d -dimensional vector of ones ;

(b) Newton's method to update \mathbf{m}_{ig} is

$$\begin{aligned} \mathbf{m}_{ig}^{(t+1)} = \mathbf{m}_{ig}^{(t)} - \mathbf{S}_{ig}^{(t+1)} & \left\{ \mathbf{y}_i - \mathbf{exp} \left[\log C_i + \mathbf{m}_{ig}^{(t)} + \frac{1}{2} \text{diag} \left(\mathbf{S}_{ig}^{(t+1)} \right) \right] \right. \\ & \left. - \boldsymbol{\Sigma}_g^{-1} \left(\mathbf{m}_{ig}^{(t)} - \boldsymbol{\mu}_g \right) \right\}. \end{aligned}$$

3. Given \widehat{Z}_{ig} and the variational parameters \mathbf{m}_{ig} and \mathbf{S}_{ig} , the parameters $\boldsymbol{\pi}$ and $\boldsymbol{\mu}_g$ are updated as:

$$\begin{aligned} \widehat{\pi}_g &= \frac{\sum_{i=1}^n \widehat{Z}_{ig}}{n}, \\ \widehat{\boldsymbol{\mu}}_g &= \frac{\sum_{i=1}^n \widehat{Z}_{ig} \mathbf{m}_{ig}^{(t+1)}}{\sum_{i=1}^n \widehat{Z}_{ig}}. \end{aligned}$$

2.4 Stage 2

In Stage 2, we treat \mathbf{X} , \mathbf{U} and \mathbf{Z} as missing such that

$$\begin{aligned} Y_{ij} \mid X_{ij} = x_{ij} & \sim \text{Poisson}(\exp\{x_{ij} + \log C_i\}) \\ \mathbf{X}_i \mid \mathbf{U}_i = \mathbf{u}_i & \sim N(\boldsymbol{\mu}_g + \boldsymbol{\Lambda}_g \mathbf{u}_i, \boldsymbol{\Psi}_g), \\ \mathbf{U}_i & \sim N(\mathbf{0}_K, \mathbf{I}_K). \end{aligned}$$

Here, we use d for the dimensionality of the observed data and K as the dimensionality of the latent variable. Suppose, we have an approximating density $q_{\mathbf{x},\mathbf{u}}(\mathbf{x}_{ig}, \mathbf{u}_{ig})$, the marginal of the log of the probability mass function of $\mathbf{Y}_i | Z_{ig} = 1$ can be written as:

$$\log f(\mathbf{y}_i | Z_{ig} = 1) = F(q_{ig}, \mathbf{y}_i) + D_{KL}(q_{ig} \| f_{ig}),$$

where $D_{KL}(q_{ig} \| f_{ig}) = \int_{\mathbb{R}^p} \int_{\mathbb{R}^d} q_{\mathbf{x},\mathbf{u}}(\mathbf{x}_{ig}, \mathbf{u}_{ig}) \log \frac{q_{\mathbf{x},\mathbf{u}}(\mathbf{x}_{ig}, \mathbf{u}_{ig})}{f(\mathbf{x}_i, \mathbf{u}_i | \mathbf{y}_i, Z_{ig}=1)} d\mathbf{x}_{ig} d\mathbf{u}_{ig}$ is the Kullback-Leibler (KL) divergence between $f(\mathbf{x}_i, \mathbf{u}_i | \mathbf{y}_i, Z_{ig} = 1)$ and approximating distribution $q(\mathbf{x}_{ig}, \mathbf{u}_{ig})$, and

$$F(q_{ig}, \mathbf{y}_i) = \int_{\mathbb{R}^p} \int_{\mathbb{R}^d} \left[\log f(\mathbf{y}_i, \mathbf{x}_i, \mathbf{u}_i | Z_{ig} = 1) - \log q_{\mathbf{x},\mathbf{u}}(\mathbf{x}_{ig}, \mathbf{u}_{ig}) \right] q_{\mathbf{x},\mathbf{u}}(\mathbf{x}_{ig}, \mathbf{u}_{ig}) d\mathbf{x}_{ig} d\mathbf{u}_{ig},$$

is our evidence lower bound (ELBO) for each observation \mathbf{y}_i .

If we assume $q_{\mathbf{x},\mathbf{u}}(\mathbf{x}_{ig}, \mathbf{u}_{ig})$ to be factorable such that $q_{\mathbf{x},\mathbf{u}}(\mathbf{x}_{ig}, \mathbf{u}_{ig}) = q_{\mathbf{x}}(\mathbf{x}_{ig})q_{\mathbf{u}}(\mathbf{u}_{ig})$,

$$\begin{aligned} F(q_{ig}, \mathbf{y}_i) = & \int_{\mathbb{R}^p} \left[\int_{\mathbb{R}^d} \left[\log f(\mathbf{y}_i | \mathbf{x}_i, \mathbf{u}_i, Z_{ig} = 1) + \log f(\mathbf{x}_i | \mathbf{u}_i, Z_{ig} = 1) - \log q_{\mathbf{x}}(\mathbf{x}_i) \right] q_{\mathbf{x}}(\mathbf{x}_{ig}) d\mathbf{x}_{ig} \right] \\ & + \log f(\mathbf{u}_i | Z_{ig} = 1) - \log q_{\mathbf{u}}(\mathbf{u}_{ig}) \Big] q_{\mathbf{u}}(\mathbf{u}_{ig}) d\mathbf{u}_{ig}. \end{aligned}$$

Using the approximating density $q_{\mathbf{x}}(\mathbf{x}_{ig})$ from Stage 1 (i.e. $q_{\mathbf{x}}(\mathbf{x}_{ig}) = N(\mathbf{m}_{ig}, \mathbf{S}_{ig})$) and assuming $q_{\mathbf{u}}(\mathbf{u}_{ig}) = N(\mathbf{P}_{ig}, \mathbf{Q}_{ig})$, we get

$$\begin{aligned} F(q_{ig}, \mathbf{y}_i) = & \mathbf{m}'_{ig} \mathbf{y}_i + \sum_{j=1}^d (\log C_i) y_{ij} - \sum_{j=1}^d \left\{ e^{\log C_i + m_{igj} + \frac{1}{2} S_{ig,jj}} + \log(y_{ij}!) \right\} + \frac{1}{2} \log |\mathbf{S}_{ig}| + \frac{d}{2} \\ & - \frac{1}{2} (\mathbf{m}_{ig} - \boldsymbol{\mu}_{ig})^T \boldsymbol{\Psi}_g^{-1} (\mathbf{m}_{ig} - \boldsymbol{\mu}_{ig}) + (\mathbf{m}_{ig} - \boldsymbol{\mu}_g)^T \boldsymbol{\Psi}_g^{-1} \boldsymbol{\Lambda}_g \mathbf{P}_{ig} - \frac{1}{2} \mathbf{P}_{ig}^T \boldsymbol{\Lambda}_g^T \boldsymbol{\Psi}_g^{-1} \boldsymbol{\Lambda}_g \mathbf{P}_{ig} \\ & - \frac{1}{2} \text{tr}(\boldsymbol{\Lambda}_g^T \boldsymbol{\Psi}_g^{-1} \boldsymbol{\Lambda}_g \mathbf{Q}_{ig}) - \frac{1}{2} \text{tr}(\boldsymbol{\Psi}_g^{-1} \mathbf{S}_{ig}) - \frac{1}{2} \log |\boldsymbol{\Psi}_g| - \frac{1}{2} \mathbf{P}_{ig}^T \mathbf{P}_{ig} + \frac{1}{2} \log |\mathbf{Q}_{ig}^{-1}| \\ & - \frac{1}{2} \text{tr}(\mathbf{Q}_{ig}) + \frac{K}{2}. \end{aligned}$$

The variational parameters \mathbf{P}_{ig} and \mathbf{Q}_{ig} that maximize this ELBO will also minimize the KL divergence. Therefore, in Stage 2, we update variational parameters \mathbf{P}_{ig} and \mathbf{Q}_{ig} , and model parameters $\boldsymbol{\Lambda}_g$ and $\boldsymbol{\Psi}_g$.

1. The update for the variational parameters \mathbf{P}_{ig} and \mathbf{Q}_{ig} are:

$$\begin{aligned}\widehat{\mathbf{Q}}_{ig}^{(t+1)} &= (\mathbf{I}_p + \widehat{\boldsymbol{\Lambda}}_g^T \widehat{\boldsymbol{\Psi}}_g^{-1} \widehat{\boldsymbol{\Lambda}}_g)^{-1} \\ &= \mathbf{I}_p - \widehat{\boldsymbol{\beta}}_g \widehat{\boldsymbol{\Lambda}}_g \text{ (after a bit of simplification where } \widehat{\boldsymbol{\beta}}_g = \widehat{\boldsymbol{\Lambda}}_g^T (\widehat{\boldsymbol{\Psi}}_g + \widehat{\boldsymbol{\Lambda}}_g \widehat{\boldsymbol{\Lambda}}_g^T)^{-1} \text{)}. \\ \widehat{\mathbf{P}}_{ig}^{(t+1)} &= \widehat{\mathbf{Q}}_{ig}^{(t+1)} \widehat{\boldsymbol{\Lambda}}_g^T \widehat{\boldsymbol{\Psi}}_g^{-1} (\mathbf{m}_{ig}^{(t+1)} - \widehat{\boldsymbol{\mu}}_g) \\ &= \widehat{\boldsymbol{\beta}}_g (\mathbf{m}_{ig}^{(t+1)} - \widehat{\boldsymbol{\mu}}_g).\end{aligned}$$

2. The update for $\boldsymbol{\Psi}_g$ and $\boldsymbol{\Lambda}_g$ are obtained by repeating the following steps until convergence:

$$\begin{aligned}\widehat{\boldsymbol{\Theta}}_g &= \mathbf{I}_p - \widehat{\boldsymbol{\beta}}_g \widehat{\boldsymbol{\Lambda}}_g + \widehat{\boldsymbol{\beta}}_g \mathbf{W}_g \widehat{\boldsymbol{\beta}}_g^T, \\ \widehat{\boldsymbol{\beta}}_g &= \widehat{\boldsymbol{\Lambda}}_g^T (\widehat{\boldsymbol{\Lambda}}_g \widehat{\boldsymbol{\Lambda}}_g^T + \widehat{\boldsymbol{\Psi}}_g)^{-1}, \\ \widehat{\boldsymbol{\Lambda}}_g &= \mathbf{W}_g \widehat{\boldsymbol{\beta}}_g^T \widehat{\boldsymbol{\Theta}}_g^{-1},\end{aligned}\tag{1}$$

$$\widehat{\boldsymbol{\Psi}}_g = \text{diag} \left(\mathbf{W}_g - \widehat{\boldsymbol{\Lambda}}_g \widehat{\boldsymbol{\beta}}_g \mathbf{W}_g + \frac{\sum_{i=1}^n \widehat{Z}_{ig} \mathbf{S}_{ig}}{\sum_{i=1}^n \widehat{Z}_{ig}} \right),\tag{2}$$

where $\mathbf{W}_g = \frac{\sum_{i=1}^n \widehat{Z}_{ig} (\mathbf{m}_{ig}^{(t+1)} - \widehat{\boldsymbol{\mu}}_g) (\mathbf{m}_{ig}^{(t+1)} - \widehat{\boldsymbol{\mu}}_g)^T}{\sum_{i=1}^n \widehat{Z}_{ig}}$ Note: convergence is assumed when the difference in Frobenius norm of $\widehat{\boldsymbol{\Lambda}}_g$ and $\widehat{\boldsymbol{\Psi}}_g$ from successive iterations are both less than 10^{-6} .

3 Family of models

To obtain a family of parsimonious models, constraints can be imposed on $\boldsymbol{\Lambda}_g$ and $\boldsymbol{\Psi}_g$ as described in Table 1 that results in a family of 8 models.

Table 1: Family of models based on the constraints on $\boldsymbol{\Lambda}_g$ and $\boldsymbol{\Psi}_g$.

Model ID	Loading Matrix $\boldsymbol{\Lambda}_g$	Error Variance $\boldsymbol{\Psi}_g$	Isotropic $\psi_g \mathbf{I}$	Covariance parameters
UUU	unconstrained	unconstrained	unconstrained	$G [dK - K(K-1)/2] + Gd$
UUC	unconstrained	unconstrained	constrained	$G [dK - K(K-1)/2] + G$
UCU	unconstrained	constrained	unconstrained	$G [dK - K(K-1)/2] + d$
UCC	unconstrained	constrained	constrained	$G [dK - K(K-1)/2] + 1$
CUU	constrained	unconstrained	unconstrained	$[dK - K(K-1)/2] + Gd$
CUC	constrained	unconstrained	constrained	$[dK - K(K-1)/2] + G$
CCU	constrained	constrained	unconstrained	$[dK - K(K-1)/2] + d$
CCC	constrained	constrained	constrained	$[dK - K(K-1)/2] + 1$

The estimation of $\boldsymbol{\Psi}_g$ and $\boldsymbol{\Lambda}_g$ under various constraints are provided below:

- Under the isotropic constraint (i.e. $\Psi_g = \psi_g \mathbf{I}_d$),

$$\hat{\psi}_g = \frac{1}{d} \text{tr} \left(\mathbf{W}_g - \hat{\Lambda}_g \hat{\beta}_g \mathbf{W}_g + \frac{\sum_{i=1}^n z_{ig} \mathbf{S}_{ig}}{n_g} \right). \quad (3)$$

- Under the equal variance constraint (i.e., $\Psi_g = \Psi$),

$$\hat{\Psi} = \text{diag} \left(\sum_{g=1}^G \frac{n_g}{n} \mathbf{W}_g - \sum_{g=1}^G \frac{n_g}{n} \hat{\Lambda}_g \hat{\beta}_g \mathbf{W}_g + \frac{1}{n} \sum_{g=1}^G \sum_{i=1}^n z_{ig} \mathbf{S}_{ig} \right).$$

- Under the equal Variance and isotropic constraint (i.e., $\Psi_g = \psi \mathbf{I}_d$),

$$\hat{\psi} = \frac{1}{d} \text{tr} \left(\sum_{g=1}^G \frac{n_g}{n} \mathbf{W}_g - \sum_{g=1}^G \frac{n_g}{n} \hat{\Lambda}_g \hat{\beta}_g \mathbf{W}_g + \frac{1}{n} \sum_{g=1}^G \sum_{i=1}^n z_{ig} \mathbf{S}_{ig} \right). \quad (4)$$

- Under the equal loading matrices constraint (i.e. $\Lambda_g = \Lambda$), the loading matrix cannot be solved directly and must be solved in a row-by-row manner as suggested by McNicholas and Murphy (2008). Hence,

$$\hat{\lambda}_i = \mathbf{r}_i \left(\sum_{g=1}^G \frac{n_g}{\hat{\Psi}_{g,(i)}} \hat{\Theta}_g \right)^{-1}, \quad (5)$$

where λ_i is the i^{th} row of the matrix Λ , $\Psi_{g,(i)}$ is the i^{th} diagonal element of Ψ_g and \mathbf{r}_i is the i^{th} row of the matrix $\sum_{g=1}^G n_g \hat{\Psi}_g^{-1} \mathbf{W}_g \hat{\beta}_g^T$.

Full details of the parameter updates for all models can be found in Appendix A.3.

4 Results

4.1 Simulation Study

Simulation studies were conducted to illustrate the ability to recover the true underlying parameters by the MPLNFA. Three simulation settings were utilized, each from a different model in the family of models. Within the three settings, three different numbers of clusters and latent factors were utilized and 100 datasets were generated with 1,000 observations per dataset under each setting. The exact specifications of the simulation settings are summarized in Table 2.

For the simulation data analyses, the normalization factors representing library size estimate for samples were set to 1. All simulation analyses were performed with R version 4.2.2 Patched ‘‘Innocent and Trusting’’, released on November 11, 2022, (R Core Team, 2022).

Table 2: Summary of the simulation settings.

Setting	Number of Simulated Datasets	Number of n Observations, n	Dimensions, d	True Model
1	100	1000	8	UCC
2	100	1000	10	CCC
3	100	1000	10	UUU

Setting	Number of Clusters, G	Mixing Proportion, π	Number of Latent factors, K	True Model
1	4	(0.11, 0.43, 0.24, 0.22)	2	UCC
2	2	(0.32, 0.68)	3	CCC
3	3	(0.23, 0.44, 0.33)	4	UUU

We fitted all the proposed eight models from the MPLNFA family to all datasets for $G = 1$ to $G_o + 1$, where G_o is the actual number of clusters and the number of latent factors ranged $K = 1$ to $K_o + 1$, where K_o is the actual number of latent factors. All models were initialized with k -means initialization with three random starts.

The simulations demonstrated that our proposed method can recover the correct parameters for MPLNFA (see Table 3). The clustering results obtained using the BIC for model selection and the corresponding average ARI values are summarized in Table 4. As seen in Table 4, BIC selected the correct number of clusters, latent factors, and component scale matrix for the first simulation setting, with $M = \text{UCC}$, with an average ARI value of 0.99. BIC provides similar results for settings 2 and 3 ($M = \text{CCC}$ and UUU , respectively), with an average ARI value of 1.00.

Additionally, in Table 4, we clustered the same data with two other common approaches, also using BIC for model selection. The first, labelled ‘mPoisson’ in Table 4, is a mixture of Poisson distributions via the `HTSCluster` R package (version 2.0.10) (Rau et al., 2015). This approach performed well in the fully constrained setting (i.e., simulation setting 2), with an average ARI of 1.00. However, it faltered with settings 1 and 3, where unconstrained elements were introduced. For settings 1 and 3, the average ARI of this approach was 0.51 and 0.69, respectively. Further, it consistently selected models with more groups than the actual number in the simulated datasets. These results were anticipated as a known limitation of this approach is that it cannot account for overdispersion, so to capture the larger variability, it will use additional components. The second approach is a mixture of Negative Binomial distributions, implemented via the `MBCluster.Seq` R package (version 1.0) and labelled ‘mNB’ in Table 4 (Si et al., 2014). This approach works very well on simulation setting 2, with an average ARI of 1.00 and identifies the correct number of groups, but it does not perform well on the other two settings. In Simulation setting 1, it has an average ARI of 0.36 and two fewer groups than the true number of groups, and in setting 3, it has an average ARI of 0.52 despite selecting the correct number of groups. A limitation of this approach is that it assumes independence between variables, and therefore cannot account for correlation, which greatly hinders its performance. As seen in these results, our

Table 3: Comparison of true and recovered parameters for all three simulation settings.

Simulation Setting 1 - UCC		
Group 1	μ	(6, 3, 3, 6, 3, 6, 3, 3)
	$\hat{\mu}$	(5.99, 3.00, 3.00, 6.00, 3.00, 6.00, 3.00, 3.00)
	Standard Deviation	(0.07, 0.10, 0.08, 0.13, 0.08, 0.07, 0.10, 0.08)
	MSE(Σ)	0.01
Group 2	μ	(1, 3, 5, 1, 3, 5, 3, 5)
	$\hat{\mu}$	(1.44, 2.85, 5.14, 1.42, 2.86, 5.15, 3.14, 4.86)
	Standard Deviation	(1.05, 0.36, 0.36, 1.04, 0.35, 0.35, 0.36, 0.35)
	MSE(Σ)	0.07
Group 3	μ	(4, 2, 6, 4, 2, 6, 4, 4)
	$\hat{\mu}$	(3.58, 2.16, 5.86, 3.59, 2.14, 5.86, 3.87, 4.13)
	Standard Deviation	(1.03, 0.34, 0.36, 1.05, 0.36, 0.36, 0.36, 0.35)
	MSE(Σ)	0.07
Group 4	μ	(5, 3, 5, 3, 5, 3, 3, 5)
	$\hat{\mu}$	(5.00, 2.99, 4.99, 3.00, 5.00, 3.01, 3.00, 5.00)
	Standard Deviation	(0.04, 0.05, 0.05, 0.05, 0.03, 0.04, 0.03, 0.06)
	MSE(Σ)	0.00
Simulation Setting 2 - CCC		
Group 1	μ	(6, 3, 3, 6, 3, 6, 3, 3, 6, 3)
	$\hat{\mu}$	(6.00, 3.00, 3.00, 6.00, 3.00, 6.01, 3.00, 3.00, 6.00, 3.00)
	Standard Deviation	(0.05, 0.07, 0.05, 0.07, 0.05, 0.05, 0.07, 0.06, 0.05, 0.06)
	MSE(Σ)	0.00
Group 2	μ	(5, 3, 5, 3, 5, 5, 3, 5, 3, 5)
	$\hat{\mu}$	(4.99, 3.01, 5.00, 3.00, 5.00, 5.00, 3.01, 5.00, 3.00, 5.00)
	Standard Deviation	(0.03, 0.05, 0.04, 0.04, 0.04, 0.04, 0.04, 0.05, 0.03, 0.05)
	MSE(Σ)	0.00
Simulation Setting 3 - UUU		
Group 1	μ	(4, 6, 4, 2, 2, 4, 6, 4, 6, 2)
	$\hat{\mu}$	(4.00, 6.00, 4.00, 1.99, 2.00, 4.00, 5.98, 4.00, 6.00, 2.00)
	Standard Deviation	(0.05, 0.10, 0.06, 0.12, 0.07, 0.07, 0.09, 0.08, 0.09, 0.08)
	MSE(Σ)	0.01
Group 2	μ	(5, 5, 3, 3, 7, 5, 3, 3, 7, 7)
	$\hat{\mu}$	(5.00, 5.00, 2.99, 3.00, 7.00, 5.00, 3.00, 3.00, 7.00, 7.00)
	Standard Deviation	(0.04, 0.07, 0.07, 0.07, 0.04, 0.03, 0.08, 0.06, 0.06, 0.07)
	MSE(Σ)	0.02
Group 3	μ	(2, 4, 4, 7, 2, 4, 7, 2, 7, 4)
	$\hat{\mu}$	(1.99, 3.99, 3.99, 6.99, 1.98, 4.00, 7.01, 1.97, 6.99, 4.00)
	Standard Deviation	(0.09, 0.06, 0.08, 0.08, 0.09, 0.07, 0.09, 0.07, 0.10, 0.07)
	MSE(Σ)	0.01

Table 4: Model selection results of the clusters (average ARI, standard deviation), latent factors and component scale matrices for each simulation setting compared to true values.

Setting	Cluster, G				Latent factor, K				Component scale matrix, M			
	Original	MPLNFA	mPoisson	mNB	Original	MPLNFA	mPoisson	mNB	Original	MPLNFA	mPoisson	mNB
1	4	4	5	2	2	2	NA	NA	UCC	UCC	NA	NA
		(0.99, 0.01)	(0.51, 0.08)	(0.36, 0.19)								
2	2	2	3	2	3	3	NA	NA	CCC	CCC	NA	NA
		(1.00, 0.00)	(1.00, 0.00)	(1.00, 0.00)								
3	3	3	4	3	4	4	NA	NA	UUU	UUU	NA	NA
		(1.00, 0.00)	(0.69, 0.02)	(0.52, 0.11)								

proposed MPLNFA model performed the best for all simulation settings due to its ability to account for overdispersion and both positive and negative correlation, both of which are known limitations of the other two compared approaches.

4.2 Transcriptome Data Analysis

To illustrate the applicability of the MPLNFA model, it was applied to a publicly available, curated RNA sequencing dataset of breast invasive carcinoma (BRCA_RNASeqGene-20160128) from The Cancer Genome Atlas (TCGA) Program (Ramos et al., 2020). Breast cancer is a commonly diagnosed cancer and a leading cause of cancer-related deaths in women worldwide (Wilkinson and Gathani, 2022). Clustering has been applied to understand breast cancer, by clustering of genes to identify co-expression networks, or clustering of tissues to identify subtypes (Sørliie et al., 2001; Kreike et al., 2007). The original dataset explored here had 878 patient tissues and 20,502 genes. The status of the estrogen receptor (ER), progesterone receptor (PR), and human epidermal growth factor receptor 2 (HER2) play a crucial role in breast cancer and its clinical management (Chen et al., 2022). Here, we focused only on a subset of tissues for which hormone receptor status was available and were females, resulting in a sample size of 712 tissues. Typically, only a subset of genes from the experiment are used for analysis purposes in order to reduce noise. The original number of 20,502 genes in the dataset was filtered to remove genes with missing expression values, resulting in 17,586 genes. The top 50 genes with the most variable gene expression across the 712 tissues were selected. The final dataset had a size of 712 tissues with 50 genes.

In terms of patient characterization, cohort ages ranged from 26 to 90, with no age data available for 9%. In terms of the pathologic stage, tissues from 11 stages (stages i, ia, ib, ii, iia, iib, iiaa, iiib, iiic, iv, x) were present, with no data for 0.98%. Staging quantifies the amount of cancer in the body, with a higher stage number indicating more cancer spread (Cuthrell and Tzenios, 2023). Stage x indicates that the status cannot be determined. A majority of the cohort was identified as white (74%), followed by black (8%), Asian (7%), American Indian or Alaska Native (0.15%), with no data available for 10.85%. In the cohort, 76.5% were ER-positive and 66.7% were PR-positive. In terms of HER2, 80.7% were negative, 13.8% were positive, 1.1% were equivocal and 1.8% did not have data. All patients were

female.

In order to identify subtypes of breast invasive carcinoma, the tissues were clustered for a clustering range from $G = 1$ to 8, and a latent factor range of $k = 1$ to 10, for all eight models listed in Table 1. All data analyses were performed using k -means initialization with 3 runs. Both BIC and ICL selected a model with $G = 5$, $k = 6$ and $M = \text{CUU}$. The 5 clusters analyzed here are interchangeably referred to as the 5 subtypes of breast invasive carcinoma. It was observed that the tissues were assigned to clusters with high posterior probabilities via the MPLNFA model (see Additional Figure 1). In this model, Clusters 1–5 were composed of 201(28%), 118(17%), 83(12%), 61(8%), and 249(35%) tissues, respectively. See Additional File 1 for the tissue composition of each cluster. In simulation studies, where the true labels are available, the ARI can be used to assess clustering performance. Because no true labels are available in real data, the predicted clusters were assessed in terms of overall survival, clinical characteristics and gene expression patterns. The distinct expression patterns between the 5 clusters are provided in Figure 1 (Gu, 2022). The genetic subtypes were associated with a divergent overall survival (OS) in the overall cohort ($P < 0.0001$) as shown in Figure 2. The most favourable OS was observed for Cluster 2 and the most unfavourable OS was observed in Clusters 4, followed by 3. In terms of race, age and pathologic stage, no significant associations were identified with the clusters. However, it was interesting to note that all races were represented in Cluster 4 and Cluster 4 also had the least proportion of tissues from stage i.

The ER and PR positive status has shown to be associated with favourable patient outcomes (Davey et al., 2021). Interestingly, Cluster 4 and Cluster 2, both contained the highest number of ER and PR negative cases. However, among all clusters, Cluster 4 contained the highest number of HER2 positive cases, while Cluster 2 had the most HER2 negative cases. HER2 overexpression or HER2 positive status in breast cancer has shown to be associated with poor prognosis and decreased survival (Chen et al., 2022). The PR is an estrogen-regulated gene, so ER-positive tumours are generally PR positive, and ER-negative tumours are PR negative (Bae et al., 2015). This is observed across clusters in the current analysis. Further, the ER positive, PR positive status is known to have a better prognosis compared to ER negative, PR negative status (Bae et al., 2015). This is evident for Cluster 1 and 5, where the majority of cases have both receptors positive.

To explore expression patterns, 50 genes in the dataset were divided into non-exclusive, three groups: developmental-related, metabolism and enzymatic-related or neurological-related genes. Cluster 1-3, and 5 showed variable expression levels among the three gene groups. However, Cluster 4 stood out as having high expression in developmental-related genes, followed by a mixed expression in metabolism-related genes, and low expression in neurological-related genes. The expression patterns observed here were supported in the literature. We selected some genes to illustrate this. For example, within development-related genes, *NKAIN1* has high expression across all clusters. This gene encodes the sodium/potassium transporting ATPase interacting with 1 protein in humans. An association between high expression of *NKAIN1* and breast cancer has been shown and *NKAIN1*

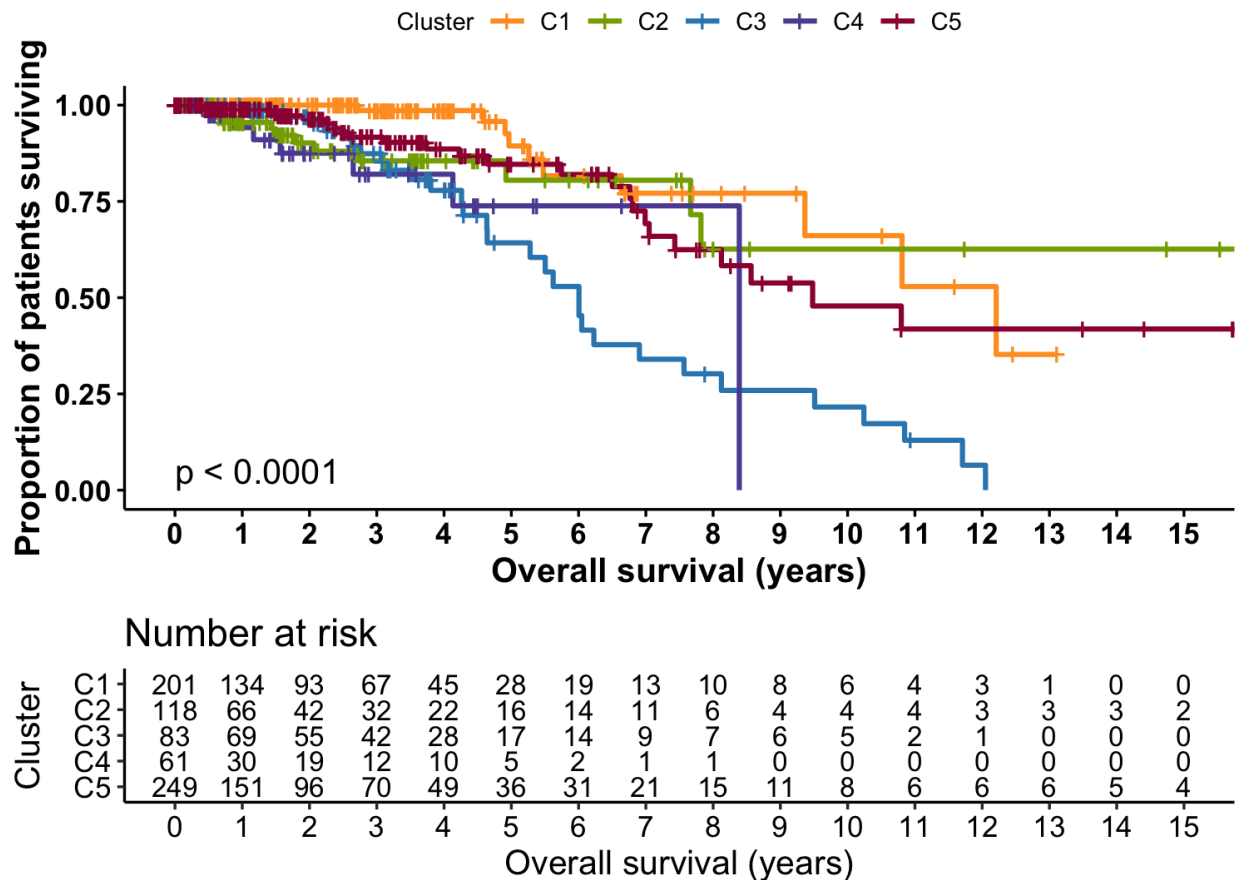


Figure 2: Kaplan-Meier plot of overall survival for Cluster 1 (C1) through Cluster 5 (C5) for the $G = 5, k = 6$ and $M = \text{CUU}$ model selected by both BIC and ICL for the breast invasive carcinoma RNA-seq dataset.

has been shown to suppress the growth of breast cancer cells and xenograft tumours (Han et al., 2018). Interestingly, Cluster 4 showed low expression of *ZIC1* and Cluster 2 showed a high expression, supporting the OS differences observed.

5 Discussion

A mixture of factor analyzers model for MPLN distribution as well as a family of mixture models based theorem is introduced. This is the first use of a mixture of MPLN factor analyzer distributions within the literature. To our knowledge, this is also the first use of a mixture of discrete factor analyzers within the literature. The proposed models are well-

suited to high-dimensional applications as the number of scale parameters is linear in data dimensionality for all eight models, as opposed to in traditional MPLN, where the parameters grow quadratically. Further, a single MPLN factor analysis model can be obtained as a special case of the mixture of MPLNFA, i.e., with $G = 1$. Extensions applicable to factor analyzers model, such as the mixture of common factor analyzers (Baek et al., 2010) can be applied to the MPLNFA family in future. A mixture of common factor analyzers is a restrictive form of the mixture of factor analyzers model and can be useful when the number of clusters and dimensionality are very large.

Overall, applying MPLNFA identified 5 subtypes of breast invasive carcinoma that differ from each other in terms of patient survival outcomes, clinical covariates and gene expression. Connecting gene expression patterns with clinical covariates and patient outcomes is important in understanding disease diversity. Findings from our study provide a deeper understanding of the molecular and clinical heterogeneity of breast cancer and these may inform the development of subtype-specific treatment strategies to improve patient outcomes in future.

Acknowledgments

This research was supported by the Postdoctoral Fellowship award from the Canadian Institutes of Health Research (Silva), the National Sciences and Engineering Research Council of Canada grant (2021-03812 - Subedi, 2023-06030 - McNicholas), and the Canada Research Chair Program (22020-00303 - Subedi, 2022-00494 - McNicholas).

5.1 Software availability

The GitHub R package for this work is available at:

<https://github.com/anjalisilva/mixMPLNFA> and is released under the open source MIT license.

A Appendix

A.1 Variational Approximations

The marginal log-density of $\mathbf{Y}_i \mid Z_{ig} = 1$ in Stage 1 can be written as:

$$\begin{aligned}
\log f(\mathbf{y}_i \mid Z_{ig} = 1) &= \int_{\mathbb{R}^d} \log f(\mathbf{y}_i \mid Z_{ig} = 1) q(\mathbf{x}_{ig}) d\mathbf{x}_{ig} \\
&= \int_{\mathbb{R}^d} \log \frac{f(\mathbf{y}_i, \mathbf{x}_i \mid Z_{ig} = 1)/q(\mathbf{x}_{ig})}{f(\mathbf{x}_i \mid \mathbf{y}_i, Z_{ig} = 1)/q(\mathbf{x}_{ig})} q(\mathbf{x}_{ig}) d\mathbf{x}_{ig} \\
&= \int_{\mathbb{R}^d} [\log f(\mathbf{y}_i, \mathbf{x}_i \mid Z_{ig} = 1) - \log q(\mathbf{x}_{ig})] q(\mathbf{x}_{ig}) d\mathbf{x}_{ig} + D_{KL}(q_{ig} \parallel f_{ig}) \\
&= F(q_{ig}, \mathbf{y}_i) + D_{KL}(q_{ig} \parallel f_{ig}),
\end{aligned}$$

The marginal log-density of $\mathbf{Y}_i \mid Z_{ig} = 1$ in Stage 2 can be written as:

$$\begin{aligned}
\log f(\mathbf{y}_i \mid Z_{ig} = 1) &= \int_{\mathbb{R}^K} \int_{\mathbb{R}^d} \log f(\mathbf{y}_i \mid Z_{ig} = 1) q_{\mathbf{x}, \mathbf{u}}(\mathbf{x}_{ig}, \mathbf{u}_{ig}) d\mathbf{x}_{ig} d\mathbf{u}_{ig} \\
&= \int_{\mathbb{R}^K} \int_{\mathbb{R}^d} \log \frac{f(\mathbf{y}_i, \mathbf{x}_i, \mathbf{u}_i \mid Z_{ig} = 1)/q_{\mathbf{x}, \mathbf{u}}(\mathbf{x}_{ig}, \mathbf{u}_{ig})}{f(\mathbf{x}_i, \mathbf{u}_i \mid \mathbf{y}_i, Z_{ig} = 1)/q_{\mathbf{x}, \mathbf{u}}(\mathbf{x}_{ig}, \mathbf{u}_{ig})} q_{\mathbf{x}, \mathbf{u}}(\mathbf{x}_{ig}, \mathbf{u}_{ig}) d\mathbf{x}_{ig} d\mathbf{u}_{ig} \\
&= \int_{\mathbb{R}^K} \int_{\mathbb{R}^d} \left[\log f(\mathbf{y}_i, \mathbf{x}_i, \mathbf{u}_i \mid Z_{ig} = 1) - \log q_{\mathbf{x}, \mathbf{u}}(\mathbf{x}_{ig}, \mathbf{u}_{ig}) \right] \\
&\quad \times q_{\mathbf{x}, \mathbf{u}}(\mathbf{x}_{ig}, \mathbf{u}_{ig}) d\mathbf{x}_{ig} d\mathbf{u}_{ig} + D_{KL}(q_{ig} \parallel f_{ig}) \\
&= F(q_{ig}, \mathbf{y}_i) + D_{KL}(q_{ig} \parallel f_{ig}),
\end{aligned}$$

ELBO in Stage 2 under the assumption that $q_{x,u}(\mathbf{x}, \mathbf{u})$ is factorable:

$$\begin{aligned}
F(q_{ig}, \mathbf{y}_i) &= \int_{\mathbb{R}^K} \int_{\mathbb{R}^d} \left[\log f(\mathbf{y}_i \mid \mathbf{x}_i, \mathbf{u}_i, Z_{ig} = 1) + \log f(\mathbf{x}_i \mid \mathbf{u}_i, Z_{ig} = 1) + \log f(\mathbf{u}_i \mid Z_{ig} = 1) \right. \\
&\quad \left. - \log q_{\mathbf{x}}(\mathbf{x}_{ig}) - \log q_{\mathbf{u}}(\mathbf{u}_{ig}) \right] q_{\mathbf{x}}(\mathbf{x}_{ig}) q_{\mathbf{u}}(\mathbf{u}_{ig}) d\mathbf{x}_{ig} d\mathbf{u}_{ig} \\
&= \int_{\mathbb{R}^K} \left[\left\{ \int_{\mathbb{R}^d} \left[\log f(\mathbf{y}_i \mid \mathbf{x}_i, \mathbf{u}_i, Z_{ig} = 1) + \log f(\mathbf{x}_i \mid \mathbf{u}_i, Z_{ig} = 1) \right. \right. \right. \\
&\quad \left. \left. - \log q_{\mathbf{x}}(\mathbf{x}_i) \right] q_{\mathbf{x}}(\mathbf{x}_{ig}) d\mathbf{x}_{ig} \right\} + \log f(\mathbf{u}_i \mid Z_{ig} = 1) - \log q_{\mathbf{u}}(\mathbf{u}_{ig}) \right] q_{\mathbf{u}}(\mathbf{u}_{ig}) d\mathbf{u}_{ig}.
\end{aligned}$$

Assuming that the approximating distributions (i.e. $q_{\mathbf{x}}(\mathbf{x}_{ig}) = N(\mathbf{m}_{ig}, \mathbf{S}_{ig})$ and $q_{\mathbf{u}}(\mathbf{u}_{ig}) =$

$N(\mathbf{P}_{ig}, \mathbf{Q}_{ig})$, the ELBO in Stage 2 becomes:

$$\begin{aligned}
F(q_{ig}, \mathbf{y}_i) &= \int_{\mathbb{R}^K} \left[\mathbf{m}'_{ig} \mathbf{y}_i + \sum_{j=1}^d (\log k_j) y_{ij} - \sum_{j=1}^d \left\{ e^{\log k_j + m_{igj} + \frac{1}{2} S_{ig,jj}} + \log(y_{ij}!) \right\} \right. \\
&\quad + \frac{1}{2} \log |\mathbf{S}_{ig}| + \frac{d}{2} - \frac{1}{2} (\mathbf{m}_{ig} - \boldsymbol{\mu}_g - \boldsymbol{\Lambda}_g \mathbf{u}_i)' \boldsymbol{\Psi}_g^{-1} (\mathbf{m}_{ig} - \boldsymbol{\mu}_g - \boldsymbol{\Lambda}_g \mathbf{u}_i) - \frac{1}{2} \text{tr} (\boldsymbol{\Psi}_g^{-1} \mathbf{S}_{ig}) \\
&\quad \left. - \frac{1}{2} \log |\boldsymbol{\Psi}_g| + \log f(\mathbf{u}_i | Z_{ig} = 1) - \log q_{\mathbf{u}}(\mathbf{u}_{ig}) \right] q_{\mathbf{u}}(\mathbf{u}_{ig}) d\mathbf{u}_{ig} \\
&= \mathbf{m}'_{ig} \mathbf{y}_i + \sum_{j=1}^d (\log k_j) y_{ij} - \sum_{j=1}^d \left\{ e^{\log k_j + m_{igj} + \frac{1}{2} S_{ig,jj}} + \log(y_{ij}!) \right\} + \frac{1}{2} \log |\mathbf{S}_{ig}| + \frac{d}{2} \\
&\quad - \frac{1}{2} (\mathbf{m}_{ig} - \boldsymbol{\mu}_{ig})^T \boldsymbol{\Psi}_g^{-1} (\mathbf{m}_{ig} - \boldsymbol{\mu}_{ig}) + (\mathbf{m}_{ig} - \boldsymbol{\mu}_g)^T \boldsymbol{\Psi}_g^{-1} \boldsymbol{\Lambda}_g \mathbf{P}_{ig} - \frac{1}{2} \mathbf{P}_{ig}^T \boldsymbol{\Lambda}_g^T \boldsymbol{\Psi}_g^{-1} \boldsymbol{\Lambda}_g \mathbf{P}_{ig} \\
&\quad - \frac{1}{2} \text{tr} (\boldsymbol{\Lambda}_g^T \boldsymbol{\Psi}_g^{-1} \boldsymbol{\Lambda}_g \mathbf{Q}_{ig}) - \frac{1}{2} \text{tr} (\boldsymbol{\Psi}_g^{-1} \mathbf{S}_{ig}) - \frac{1}{2} \log |\boldsymbol{\Psi}_g| - \frac{1}{2} \mathbf{P}_{ig}^T \mathbf{P}_{ig} + \frac{1}{2} \log |\mathbf{Q}_{ig}^{-1}| \\
&\quad - \frac{1}{2} \text{tr}(\mathbf{Q}_{ig}) + \frac{K}{2}.
\end{aligned}$$

A.2 Family of Models

A.2.1 Isotropic assumption: $\boldsymbol{\Psi}_g = \psi_g \mathbf{I}_d$

$$\begin{aligned}
l(\boldsymbol{\vartheta}) &= \sum_{g=1}^G \sum_{i=1}^n z_{ig} \log \pi_g + \sum_{g=1}^G \sum_{i=1}^n z_{ig} \log f(\mathbf{y}_i | Z_{ig} = 1, \boldsymbol{\mu}_g, \boldsymbol{\Psi}_g, \boldsymbol{\Lambda}_g). \\
&= \sum_{g=1}^G \sum_{i=1}^n z_{ig} \log \pi_g + \sum_{g=1}^G \sum_{i=1}^n z_{ig} \{F(q_{ig}, \mathbf{y}_i) + D_{KL}(q_{ig} || f_{ig})\}
\end{aligned}$$

Under the isotropic constraint (i.e. $\mathbf{\Psi}_g = \psi_g \mathbf{I}_d$),

$$\begin{aligned}
\sum_{g=1}^G \sum_{i=1}^n z_{ig} F(q_{ig}, \mathbf{y}_i) &= \sum_{g=1}^G \sum_{i=1}^n z_{ig} \left[-\frac{\psi_g^{-1}}{2} (\mathbf{m}_{ig} - \boldsymbol{\mu}_{ig})^T (\mathbf{m}_{ig} - \boldsymbol{\mu}_{ig}) + \psi_g^{-1} (\mathbf{m}_{ig} - \boldsymbol{\mu}_{ig})^T \boldsymbol{\Lambda}_g \mathbf{P}_{ig} \right. \\
&\quad \left. + \frac{d}{2} \log \psi_g^{-1} - \frac{\psi_g^{-1}}{2} \mathbf{P}_{ig}^T \boldsymbol{\Lambda}_g^T \boldsymbol{\Lambda}_g \mathbf{P}_{ig} - \frac{\psi_g^{-1}}{2} \text{tr}(\boldsymbol{\Lambda}_g^T \boldsymbol{\Lambda}_g \mathbf{Q}_g) - \frac{\psi_g^{-1}}{2} \text{tr}(\mathbf{S}_{ig}) \right] + C, \\
&= \sum_{g=1}^G \left[-\frac{\psi_g^{-1}}{2} n_g \text{tr}(\mathbf{W}_g) + \psi_g^{-1} n_g \text{tr}(\mathbf{W}_g \boldsymbol{\Lambda}_g \boldsymbol{\beta}_g) + \frac{dn_g}{2} \log \psi_g^{-1} \right. \\
&\quad - \frac{\psi_g^{-1} n_g}{2} \text{tr}(\boldsymbol{\Lambda}_g^T \boldsymbol{\Lambda}_g \mathbf{Q}_g) - \frac{\psi_g^{-1}}{2} n_g \text{tr}(\boldsymbol{\beta}_g^T \boldsymbol{\Lambda}_g^T \boldsymbol{\Lambda}_g \boldsymbol{\beta}_g \mathbf{W}_g) \\
&\quad \left. - \frac{\psi_g^{-1}}{2} \text{tr} \left(\sum_{i=1}^n z_{ig} \mathbf{S}_{ig} \right) \right] + C,
\end{aligned}$$

where C is a constant with respect to ψ_g^{-1} and $n_g = \sum_{i=1}^n z_{ig}$. Taking derivative with respect to ψ_g^{-1} and setting it to 0, we get

$$\begin{aligned}
d\hat{\psi}_g - \text{tr}(\mathbf{W}_g) + 2 \text{tr}(\mathbf{W}_g \hat{\boldsymbol{\Lambda}}_g \hat{\boldsymbol{\beta}}_g) - \text{tr}(\hat{\boldsymbol{\beta}}_g^T \hat{\boldsymbol{\Lambda}}_g^T \hat{\boldsymbol{\Lambda}}_g \hat{\boldsymbol{\beta}}_g \mathbf{W}_g) \\
- \text{tr}(\hat{\boldsymbol{\Lambda}}_g^T \hat{\boldsymbol{\Lambda}}_g \mathbf{Q}_g) - \text{tr} \left(\frac{\sum_{i=1}^n z_{ig} \mathbf{S}_{ig}}{n_g} \right) = 0.
\end{aligned}$$

Simplifying this, we get

$$\hat{\psi}_g = \frac{1}{d} \text{tr} \left(\mathbf{W}_g - \hat{\boldsymbol{\Lambda}}_g \hat{\boldsymbol{\beta}}_g \mathbf{W}_g + \frac{\sum_{i=1}^n z_{ig} \mathbf{S}_{ig}}{n_g} \right). \tag{6}$$

A.2.2 Equal Variance: $\Psi_g = \Psi$

Under the equal variance constraint (i.e. $\Psi_g = \Psi$),

$$\begin{aligned}
\sum_{g=1}^G \sum_{i=1}^n z_{ig} F(q_{ig}, \mathbf{y}_i) &= \sum_{g=1}^G \sum_{i=1}^n z_{ig} \left[-\frac{1}{2} (\mathbf{m}_{ig} - \boldsymbol{\mu}_{ig})^T \boldsymbol{\Psi}^{-1} (\mathbf{m}_{ig} - \boldsymbol{\mu}_{ig}) \right. \\
&\quad + (\mathbf{m}_{ig} - \boldsymbol{\mu}_{ig})^T \boldsymbol{\Psi}^{-1} \boldsymbol{\Lambda}_g \mathbf{P}_{ig} + \frac{1}{2} \log |\boldsymbol{\Psi}^{-1}| - \frac{1}{2} \mathbf{P}_{ig}^T \boldsymbol{\Lambda}_g^T \boldsymbol{\Psi}^{-1} \boldsymbol{\Lambda}_g \mathbf{P}_{ig} \\
&\quad \left. - \frac{1}{2} \text{tr}(\boldsymbol{\Lambda}_g^T \boldsymbol{\Psi}^{-1} \boldsymbol{\Lambda}_g \mathbf{Q}_g) - \frac{1}{2} \text{tr}(\boldsymbol{\Psi}^{-1} \mathbf{S}_{ig}) \right] + C, \\
&= \sum_{g=1}^G \left[-\frac{n_g}{2} \text{tr}(\boldsymbol{\Psi}^{-1} \mathbf{W}_g) + n_g \text{tr}(\mathbf{W}_g \boldsymbol{\Psi}^{-1} \boldsymbol{\Lambda}_g \boldsymbol{\beta}_g) - \frac{n_g}{2} \text{tr}(\boldsymbol{\Lambda}_g^T \boldsymbol{\Psi}^{-1} \boldsymbol{\Lambda}_g \mathbf{Q}_g) \right. \\
&\quad + \frac{n_g}{2} \log |\boldsymbol{\Psi}^{-1}| - \frac{\psi_g^{-1}}{2} n_g \text{tr}(\boldsymbol{\beta}_g^T \boldsymbol{\Lambda}_g^T \boldsymbol{\Psi}^{-1} \boldsymbol{\Lambda}_g \boldsymbol{\beta}_g \mathbf{W}_g) \\
&\quad \left. - \frac{1}{2} \text{tr} \left(\boldsymbol{\Psi}^{-1} \sum_{i=1}^n z_{ig} \mathbf{S}_{ig} \right) \right] + C,
\end{aligned}$$

where C is a constant with respect to $\boldsymbol{\Psi}$ and $n_g = \sum_{i=1}^n z_{ig}$. Taking derivative with respect to $\boldsymbol{\Psi}^{-1}$ and setting it to 0, we get

$$\begin{aligned}
n \hat{\boldsymbol{\Psi}} - \sum_{g=1}^G n_g \mathbf{W}_g + 2 \sum_{g=1}^G n_g \hat{\boldsymbol{\Lambda}}_g \hat{\boldsymbol{\beta}}_g \mathbf{W}_g - \sum_{g=1}^G n_g \hat{\boldsymbol{\beta}}_g^T \hat{\boldsymbol{\Lambda}}_g^T \hat{\boldsymbol{\Lambda}}_g \hat{\boldsymbol{\beta}}_g \mathbf{W}_g \\
- \sum_{g=1}^G n_g \hat{\boldsymbol{\Lambda}}_g^T \hat{\boldsymbol{\Lambda}}_g \mathbf{Q}_g - \text{tr} \left(\frac{\sum_{i=1}^n z_{ig} \mathbf{S}_{ig}}{n_g} \right) = 0.
\end{aligned}$$

Simplifying this, we get

$$\begin{aligned}
\hat{\boldsymbol{\Psi}} &= \text{diag} \left(\sum_{g=1}^G \frac{n_g}{n} \mathbf{W}_g - \sum_{g=1}^G \frac{n_g}{n} \hat{\boldsymbol{\Lambda}}_g \hat{\boldsymbol{\beta}}_g \mathbf{W}_g + \frac{1}{n} \sum_{g=1}^G \sum_{i=1}^n z_{ig} \mathbf{S}_{ig} \right). \\
&= \text{diag} \left(\sum_{g=1}^G \frac{n_g}{n} \mathbf{W}_g - \sum_{g=1}^G \frac{n_g}{n} \hat{\boldsymbol{\Lambda}}_g \hat{\boldsymbol{\beta}}_g \mathbf{W}_g + \frac{1}{n} \sum_{g=1}^G \sum_{i=1}^n z_{ig} \mathbf{S}_{ig} \right)
\end{aligned}$$

A.2.3 Equal Variance and isotropic constraint $\Psi_g = \psi \mathbf{I}_d$

$$\begin{aligned}
\sum_{g=1}^G \sum_{i=1}^n z_{ig} F(q_{ig}, \mathbf{y}_i) &= \sum_{g=1}^G \sum_{i=1}^n z_{ig} \left[-\frac{\psi^{-1}}{2} (\mathbf{m}_{ig} - \boldsymbol{\mu}_{ig})^T (\mathbf{m}_{ig} - \boldsymbol{\mu}_{ig}) + \psi^{-1} (\mathbf{m}_{ig} - \boldsymbol{\mu}_g)^T \boldsymbol{\Lambda}_g \mathbf{P}_{ig} \right. \\
&\quad \left. + \frac{d}{2} \log \psi^{-1} - \frac{\psi^{-1}}{2} \mathbf{P}_{ig}^T \boldsymbol{\Lambda}_g^T \boldsymbol{\Lambda}_g \mathbf{P}_{ig} - \frac{\psi^{-1}}{2} \text{tr}(\boldsymbol{\Lambda}_g^T \boldsymbol{\Lambda}_g \mathbf{Q}_g) - \frac{\psi^{-1}}{2} \text{tr}(\mathbf{S}_{ig}) \right] + C, \\
&= \sum_{g=1}^G \left[-\frac{\psi^{-1}}{2} n_g \text{tr}(\mathbf{W}_g) + \psi^{-1} n_g \text{tr}(\mathbf{W}_g \boldsymbol{\Lambda}_g \boldsymbol{\beta}_g) + \frac{dn_g}{2} \log \psi^{-1} \right. \\
&\quad - \frac{\psi^{-1} n_g}{2} \text{tr}(\boldsymbol{\Lambda}_g^T \boldsymbol{\Lambda}_g \mathbf{Q}_g) - \frac{\psi^{-1}}{2} n_g \text{tr}(\boldsymbol{\beta}_g^T \boldsymbol{\Lambda}_g^T \boldsymbol{\Lambda}_g \boldsymbol{\beta}_g \mathbf{W}_g) \\
&\quad \left. - \frac{\psi^{-1}}{2} \text{tr} \left(\sum_{i=1}^n z_{ig} \mathbf{S}_{ig} \right) \right] + C,
\end{aligned}$$

where C is a constant with respect to ψ^{-1} and $n_g = \sum_{i=1}^n z_{ig}$. Taking derivative with respect to ψ^{-1} and setting it to 0, we get

$$\begin{aligned}
dn\hat{\psi} - \text{tr} \left(\sum_{g=1}^G n_g \mathbf{W}_g \right) + 2 \text{tr} \left(\sum_{g=1}^G n_g \mathbf{W}_g \hat{\boldsymbol{\Lambda}}_g \hat{\boldsymbol{\beta}}_g \right) - \text{tr} \left(\sum_{g=1}^G n_g \hat{\boldsymbol{\beta}}_g^T \hat{\boldsymbol{\Lambda}}_g^T \hat{\boldsymbol{\Lambda}}_g \hat{\boldsymbol{\beta}}_g \mathbf{W}_g \right) \\
- \text{tr} \left(\sum_{g=1}^G n_g \hat{\boldsymbol{\Lambda}}_g^T \hat{\boldsymbol{\Lambda}}_g \mathbf{Q}_g \right) - \text{tr} \left(\sum_{g=1}^G \sum_{i=1}^n z_{ig} \mathbf{S}_{ig} \right) = 0.
\end{aligned}$$

And, simplifying this, we get

$$\hat{\psi} = \frac{1}{d} \text{tr} \left(\sum_{g=1}^G \frac{n_g}{n} \mathbf{W}_g - \sum_{g=1}^G \frac{n_g}{n} \hat{\boldsymbol{\Lambda}}_g \hat{\boldsymbol{\beta}}_g \mathbf{W}_g + \frac{1}{n} \sum_{g=1}^G \sum_{i=1}^n z_{ig} \mathbf{S}_{ig} \right) \quad (7)$$

A.2.4 Equal Loading Matrices: $\boldsymbol{\Lambda}_g = \boldsymbol{\Lambda}$

Under the equal loading matrices constraint (i.e. $\boldsymbol{\Lambda}_g = \boldsymbol{\Lambda}$),

$$\begin{aligned}
\sum_{g=1}^G \sum_{i=1}^n z_{ig} F(q_{ig}, \mathbf{y}_i) &= \sum_{g=1}^G \sum_{i=1}^n z_{ig} \left((\mathbf{m}_{ig} - \boldsymbol{\mu}_g)^T \boldsymbol{\Psi}_g^{-1} \boldsymbol{\Lambda} \mathbf{P}_{ig} - \frac{1}{2} \mathbf{P}_{ig}^T \boldsymbol{\Lambda}^T \boldsymbol{\Psi}_g^{-1} \boldsymbol{\Lambda} \mathbf{P}_{ig} \right. \\
&\quad \left. - \frac{1}{2} \text{tr}(\boldsymbol{\Lambda}^T \boldsymbol{\Psi}_g^{-1} \boldsymbol{\Lambda} \mathbf{Q}_g) \right) \\
&= \sum_{g=1}^G \left(n_g \text{tr}(\boldsymbol{\beta}_g \mathbf{W}_g \boldsymbol{\Psi}_g^{-1} \boldsymbol{\Lambda}) - \frac{n_g}{2} \text{tr}(\boldsymbol{\beta}_g^T \boldsymbol{\Lambda}^T \boldsymbol{\Psi}_g^{-1} \boldsymbol{\Lambda} \boldsymbol{\beta}_g \mathbf{W}_g) \right. \\
&\quad \left. - \frac{n_g}{2} \text{tr}(\boldsymbol{\Lambda}^T \boldsymbol{\Psi}_g^{-1} \boldsymbol{\Lambda} \mathbf{Q}_g) \right).
\end{aligned}$$

Taking derivative with respect to $\mathbf{\Lambda}$ and setting it equal to 0, we get

$$\begin{aligned}
0 &= \sum_{g=1}^G n_g \hat{\Psi}_g^{-1} \mathbf{W}_g \hat{\beta}_g^T - \sum_{g=1}^G n_g \hat{\Psi}_g^{-1} \hat{\Lambda} \hat{\beta}_g \mathbf{W}_g \hat{\beta}_g^T - \sum_{g=1}^G n_g \hat{\Psi}_g^{-1} \hat{\Lambda} \mathbf{Q}_g \\
&= \sum_{g=1}^G n_g \hat{\Psi}_g^{-1} \mathbf{W}_g \hat{\beta}_g^T - \sum_{g=1}^G n_g \hat{\Psi}_g^{-1} \hat{\Lambda} \left(\hat{\beta}_g \mathbf{W}_g \hat{\beta}_g^T - \mathbf{I}_p - \hat{\beta}_g \hat{\Lambda} \right) \\
&= \sum_{g=1}^G n_g \hat{\Psi}_g^{-1} \mathbf{W}_g \hat{\beta}_g^T - \sum_{g=1}^G n_g \hat{\Psi}_g^{-1} \hat{\Lambda} \hat{\Theta}_g.
\end{aligned}$$

In this case, the loading matrix cannot be solved directly and must be solved in a row-by-row manner as suggested by McNicholas and Murphy (2008). Hence,

$$\hat{\lambda}_i = \mathbf{r}_i \left(\sum_{g=1}^G \frac{n_g}{\hat{\Psi}_{g,(i)}} \hat{\Theta}_g \right)^{-1}, \quad (8)$$

where λ_i is the i^{th} row of the matrix $\mathbf{\Lambda}$, $\Psi_{g,(i)}$ is the i^{th} diagonal element of Ψ_g and \mathbf{r}_i is the i^{th} row of the matrix $\sum_{g=1}^G n_g \hat{\Psi}_g^{-1} \mathbf{W}_g \hat{\beta}_g^T$.

A.3 Parameter Updates

Table 5: Parameter Updates for the family of models based on constraints on Λ_g and Ψ_g .

Model	Parameters	Estimates
UUU	β_g	$\hat{\beta}_g = \hat{\Lambda}_g^T (\hat{\Lambda}_g \hat{\Lambda}_g^T + \Psi_g)^{-1}$
	Θ_g	$\hat{\Theta}_g = \mathbf{I}_K - \hat{\beta}_g \hat{\Lambda}_g + \hat{\beta}_g \mathbf{W}_g \hat{\beta}_g^T$
	Λ_g	$\hat{\Lambda}_g = \mathbf{W}_g \hat{\beta}_g^T \hat{\Theta}_g^{-1}$
	Ψ_g	$\hat{\Psi}_g = \text{diag} \left(\mathbf{W}_g - \hat{\Lambda}_g \hat{\beta}_g \mathbf{W}_g + \frac{\sum_{i=1}^n \hat{Z}_{ig} \mathbf{S}_{ig}}{\sum_{i=1}^n \hat{Z}_{ig}} \right)$
UUC	β_g	$\hat{\beta}_g = \hat{\Lambda}_g^T (\hat{\Lambda}_g \hat{\Lambda}_g^T + \psi_g \mathbf{I}_d)^{-1}$
	Θ_g	$\hat{\Theta}_g = \mathbf{I}_K - \hat{\beta}_g \hat{\Lambda}_g + \hat{\beta}_g \mathbf{W}_g \hat{\beta}_g^T$
	Λ_g	$\hat{\Lambda}_g = \mathbf{W}_g \hat{\beta}_g^T \hat{\Theta}_g^{-1}$
	$\Psi_g = \psi_g \mathbf{I}_d$	$\hat{\psi}_g = \frac{1}{d} \text{tr} \left(\mathbf{W}_g - \hat{\Lambda}_g \hat{\beta}_g \mathbf{W}_g + \frac{\sum_{i=1}^n z_{ig} \mathbf{S}_{ig}}{n_g} \right)$
UCU	β_g	$\hat{\beta}_g = \hat{\Lambda}_g^T (\hat{\Lambda}_g \hat{\Lambda}_g^T + \Psi)^{-1}$
	Θ_g	$\hat{\Theta}_g = \mathbf{I}_K - \hat{\beta}_g \hat{\Lambda}_g + \hat{\beta}_g \mathbf{W}_g \hat{\beta}_g^T$
	Λ_g	$\hat{\Lambda}_g = \mathbf{W}_g \hat{\beta}_g^T \hat{\Theta}_g^{-1}$
	$\Psi_g = \Psi$	$\hat{\Psi} = \text{diag} \left(\sum_{g=1}^G \frac{n_g}{n} \mathbf{W}_g - \sum_{g=1}^G \frac{n_g}{n} \hat{\Lambda}_g \hat{\beta}_g \mathbf{W}_g + \frac{1}{n} \sum_{g=1}^G \sum_{i=1}^n z_{ig} \mathbf{S}_{ig} \right)$
UCC	β_g	$\hat{\beta}_g = \hat{\Lambda}_g^T (\hat{\Lambda}_g \hat{\Lambda}_g^T + \psi \mathbf{I})^{-1}$
	Θ_g	$\hat{\Theta}_g = \mathbf{I}_K - \hat{\beta}_g \hat{\Lambda}_g + \hat{\beta}_g \mathbf{W}_g \hat{\beta}_g^T$
	Λ_g	$\hat{\Lambda}_g = \mathbf{W}_g \hat{\beta}_g^T \hat{\Theta}_g^{-1}$
	$\Psi_g = \psi \mathbf{I}$	$\hat{\psi} = \frac{1}{d} \text{tr} \left(\sum_{g=1}^G \frac{n_g}{n} \mathbf{W}_g - \sum_{g=1}^G \frac{n_g}{n} \hat{\Lambda}_g \hat{\beta}_g \mathbf{W}_g + \frac{1}{n} \sum_{g=1}^G \sum_{i=1}^n z_{ig} \mathbf{S}_{ig} \right)$
CUU	β_g	$\hat{\beta}_g = \hat{\Lambda}^T (\hat{\Lambda} \hat{\Lambda}^T + \Psi_g)^{-1}$
	Θ_g	$\hat{\Theta}_g = \mathbf{I}_K - \hat{\beta}_g \hat{\Lambda} + \hat{\beta}_g \mathbf{W}_g \hat{\beta}_g^T$
	$\Lambda_g = \Lambda$	Updated using Equation 5.
	Ψ_g	$\hat{\Psi}_g = \text{diag} \left(\mathbf{W}_g - \hat{\Lambda} \hat{\beta}_g \mathbf{W}_g + \frac{\sum_{i=1}^n \hat{Z}_{ig} \mathbf{S}_{ig}}{\sum_{i=1}^n \hat{Z}_{ig}} \right)$
CUC	β_g	$\hat{\beta}_g = \hat{\Lambda}^T (\hat{\Lambda} \hat{\Lambda}^T + \psi_g \mathbf{I}_d)^{-1}$
	Θ_g	$\hat{\Theta}_g = \mathbf{I}_K - \hat{\beta}_g \hat{\Lambda} + \hat{\beta}_g \mathbf{W}_g \hat{\beta}_g^T$
	$\Lambda_g = \Lambda$	Updated using Equation 5.

Continued on next page...

Model	Parameters	Estimates
	$\Psi_g = \psi_g \mathbf{I}_d$	$\hat{\psi}_g = \frac{1}{d} \text{tr} \left(\mathbf{W}_g - \hat{\Lambda} \hat{\beta}_g \mathbf{W}_g + \frac{\sum_{i=1}^n z_{ig} \mathbf{S}_{ig}}{n_g} \right)$
CCU	$\beta_g = \beta$	$\hat{\beta} = \hat{\Lambda}^T (\hat{\Lambda} \hat{\Lambda}^T + \Psi)^{-1}$
	Θ_g	$\hat{\Theta}_g = \mathbf{I}_K - \hat{\beta} \hat{\Lambda} + \hat{\beta} \mathbf{W}_g \hat{\beta}^T$
	$\Lambda_g = \Lambda$	Updated using Equation 5.
	$\Psi_g = \Psi$	$\hat{\Psi} = \text{diag} \left(\sum_{g=1}^G \frac{n_g}{n} \mathbf{W}_g - \sum_{g=1}^G \frac{n_g}{n} \hat{\Lambda} \hat{\beta} \mathbf{W}_g + \frac{1}{n} \sum_{g=1}^G \sum_{i=1}^n z_{ig} \mathbf{S}_{ig} \right)$
CCC	$\beta_g = \beta$	$\hat{\beta} = \hat{\Lambda}^T (\hat{\Lambda} \hat{\Lambda}^T + \psi \mathbf{I}_d)^{-1}$
	Θ_g	$\hat{\Theta}_g = \mathbf{I}_K - \hat{\beta} \hat{\Lambda} + \hat{\beta} \mathbf{W}_g \hat{\beta}^T$
	$\Lambda_g = \Lambda$	Updated using Equation 5.
	$\Psi_g = \psi \mathbf{I}$	$\hat{\psi} = \frac{1}{d} \text{tr} \left(\sum_{g=1}^G \frac{n_g}{n} \mathbf{W}_g - \sum_{g=1}^G \frac{n_g}{n} \hat{\Lambda} \hat{\beta} \mathbf{W}_g + \frac{1}{n} \sum_{g=1}^G \sum_{i=1}^n z_{ig} \mathbf{S}_{ig} \right)$

References

- Ahn, J., M. D. Gammon, R. M. Santella, M. M. Gaudet, J. A. Britton, S. L. Teitelbaum, M. B. Terry, A. I. Neugut, S. M. Eng, Y. Zhang, C. Garza, and C. B. Ambrosone (2006, 04). Effects of glutathione S-transferase A1 (GSTA1) genotype and potential modifiers on breast cancer risk . *Carcinogenesis* 27(9), 1876–1882.
- Aitchison, J. and C. Ho (1989). The multivariate Poisson-log normal distribution. *Biometrika* 76(4), 643–653.
- Ali-Hassanzadeh, M., A. Golestan, A. Tahmasebi, and A. Ramezani (2022, May). In silico identification of nkain1 gene as a potential breast cancer associated biomarker and validation using real time pcr technique. *Journal of Jiroft University of Medical Sciences*.
- Arridge, S. R., K. Ito, B. Jin, and C. Zhang (2018). Variational gaussian approximation for poisson data. *Inverse Problems* 34(2), 025005.
- Bae, S. Y., S. Kim, J. H. Lee, H.-c. Lee, S. K. Lee, W. H. Kil, S. W. Kim, J. E. Lee, and S. J. Nam (2015). Poor prognosis of single hormone receptor-positive breast cancer: similar outcome as triple-negative breast cancer. *BMC Cancer* 15(1), 1–9.
- Baek, J., G. J. McLachlan, and L. K. Flack (2010). Mixtures of factor analyzers with common factor loadings: Applications to the clustering and visualization of high-dimensional data. *IEEE Transactions on Pattern Analysis and Machine Intelligence* 32(7), 1298–1309.
- Bouveyron, C. and C. Brunet (2012). Simultaneous model-based clustering and visualization in the fisher discriminative subspace. *Statistics and Computing* 22(1), 301–324.

- Browne, R. P. and P. D. McNicholas (2015). A mixture of generalized hyperbolic distributions. *Canadian Journal of Statistics* 43(2), 176–198.
- Chen, M., J. Wu, D. Liu, W. Chen, C. Lin, L. Andriani, S. Ding, O. Huang, J. He, X. Chen, W. Chen, Y. Li, K. Shen, and L. Zhu (2022). Combined estrogen receptor and progesterone receptor level can predict survival outcome in human epidermal growth factor receptor 2-positive early breast cancer. *Clinical Breast Cancer* 22(2), e147–e156.
- Cuthrell, K. M. and N. Tzenios (2023). Breast cancer: Updated and deep insights. *International Research Journal of Oncology* 6(1), 104–118.
- Dang, U. J., R. P. Browne, and P. D. McNicholas (2015). Mixtures of multivariate power exponential distributions. *Biometrics* 71(4), 1081–1089.
- Davey, M. G., É. J. Ryan, P. J. Folan, N. O’Halloran, M. R. Boland, M. K. Barry, K. J. Sweeney, C. M. Malone, R. J. McLaughlin, M. J. Kerin, et al. (2021). The impact of progesterone receptor negativity on oncological outcomes in oestrogen-receptor-positive breast cancer. *BJS Open* 5(3), zrab040.
- de Souto, M. C., I. G. Costa, D. S. de Araujo, T. B. Ludermir, and A. Schliep (2008). Clustering cancer gene expression data: a comparative study. *BMC Bioinformatics* 9(1), 1.
- Di, Y., D. W. Schafer, J. S. Cumbie, and J. H. Chang (2011). The nbp negative binomial model for assessing differential gene expression from rna-seq. *Statistical Applications in Genetics and Molecular Biology* 10(1).
- Ghahramani, Z., G. E. Hinton, et al. (1996). The EM algorithm for mixtures of factor analyzers. Technical report, Technical Report CRG-TR-96-1, University of Toronto.
- Gollini, I. and T. B. Murphy (2014). Mixture of latent trait analyzers for model-based clustering of categorical data. *Statistics and Computing* 24(4), 569–588.
- Gu, Z. (2022). Complex heatmap visualization. *iMeta*.
- Han, W., F. Cao, X.-J. Gao, H.-B. Wang, F. Chen, S.-J. Cai, C. Zhang, Y.-W. Hu, J. Ma, X. Gu, and et al. (2018, Sep). Zic1 acts a tumor suppressor in breast cancer by targeting survivin. *International Journal of Oncology*.
- Hand, D. J. (1989). *Journal of the Royal Statistical Society. Series C (Applied Statistics)* 38(2), 384–385.
- Iravani, O., B.-H. Bay, and G. W.-C. Yip (2017). Silencing hs6st3 inhibits growth and progression of breast cancer cells through suppressing igflr and inducing xaf1. *Experimental Cell Research* 350(2), 380–389.

- Kosmidis, I. and D. Karlis (2016). Model-based clustering using copulas with applications. *Statistics and Computing* 26(5), 1079–1099.
- Kreike, B., M. van Kouwenhove, H. Horlings, B. Weigelt, H. Peterse, H. Bartelink, and M. J. van de Vijver (2007). Gene expression profiling and histopathological characterization of triple-negative/basal-like breast carcinomas. *Breast Cancer Research* 9, 1–14.
- Lawley, D. N. and A. E. Maxwell (1962). Factor analysis as a statistical method. *Journal of the Royal Statistical Society. Series D (The Statistician)* 12(3), 209–229.
- Liu, X., X. Sui, C. Zhang, K. Wei, Y. Bao, J. Xiong, Z. Zhou, Z. Chen, C. Wang, H. Zhu, and et al. (2020, Jan). Glutathione s-transferase a1 suppresses tumor progression and indicates better prognosis of human primary hepatocellular carcinoma. *Journal of Cancer* 11.
- McLachlan, D. and D. Peel (2000). *Finite Mixture Models*. Wiley.
- McNicholas, P. D. (2016). *Mixture Model-Based Classification* (1st ed.). Chapman and Hall/CRC Press.
- McNicholas, P. D. and T. B. Murphy (2008). Parsimonious gaussian mixture models. *Statistics and Computing* 18(3), 285–296.
- McNicholas, P. D. and T. B. Murphy (2010, 08). Model-based clustering of microarray expression data via latent Gaussian mixture models. *Bioinformatics* 26(21), 2705–2712.
- Naderi, A. (2017, May). C1orf64 is a novel androgen receptor target gene and coregulator that interacts with 14-3-3 protein in breast cancer. *Oncotarget*.
- R Core Team (2022). *R: A Language and Environment for Statistical Computing*. Vienna, Austria: R Foundation for Statistical Computing.
- Ramos, M., L. Geistlinger, S. Oh, L. Schiffer, R. Azhar, H. Kodali, I. de Bruijn, J. Gao, V. J. Carey, M. Morgan, and L. Waldron (2020). Multiomic integration of public oncology databases in bioconductor. *JCO Clinical Cancer Informatics* (4), 958–971. PMID: 33119407.
- Rau, A., C. Maugis-Rabusseau, M.-L. Martin-Magniette, and G. Celeux (2015). Co-expression analysis of high-throughput transcriptome sequencing data with Poisson mixture models. *Bioinformatics* 31(9), 1420–1427.
- Roberts, A., H. Pimentel, C. Trapnell, and L. Pachter (2011). Identification of novel transcripts in annotated genomes using RNA-seq. *Bioinformatics* 27, 2325–2329.
- Si, Y., P. Liu, P. Li, and T. P. Brutnell (2014). Model-based clustering for RNA-seq data. *Bioinformatics* 30(2), 197–205.

- Silva, A., X. Qin, S. J. Rothstein, P. D. McNicholas, and S. Subedi (2023). Finite mixtures of matrix variate Poisson-log normal distributions for three-way count data. *Bioinformatics* 39(5), btad167.
- Silva, A., S. J. Rothstein, P. D. McNicholas, and S. Subedi (2019). A multivariate poisson-log normal mixture model for clustering transcriptome sequencing data. *BMC Bioinformatics* 20(1), 394.
- Sørli, T., C. M. Perou, R. Tibshirani, T. Aas, S. Geisler, H. Johnsen, T. Hastie, M. B. Eisen, M. Van De Rijn, S. S. Jeffrey, et al. (2001). Gene expression patterns of breast carcinomas distinguish tumor subclasses with clinical implications. *Proceedings of the National Academy of Sciences* 98(19), 10869–10874.
- Spearman, C. (1904). The proof and measurement of association between two things. *The American Journal of Psychology* 15(1), 72–101.
- Subedi, S. and R. Browne (2020). A parsimonious family of multivariate poisson-lognormal distributions for clustering multivariate count data. *arXiv preprint arXiv:2004.06857*.
- Subedi, S. and P. D. McNicholas (2014). Variational bayes approximations for clustering via mixtures of normal inverse gaussian distributions. *Advances in Data Analysis and Classification* 8(2), 167–193.
- Subedi, S. and P. D. McNicholas (2020). A variational approximations-dic rubric for parameter estimation and mixture model selection within a family setting. *Journal of Classification*, 1–20.
- Subedi, S., A. Punzo, S. Ingrassia, and P. D. McNicholas (2015). Cluster-weighted t -factor analyzers for robust model-based clustering and dimension reduction. *Statistical Methods & Applications* 24(4), 623–649.
- Tortora, C., B. C. Franczak, R. P. Browne, and P. D. McNicholas (2019). A mixture of coalesced generalized hyperbolic distributions. *Journal of Classification* 36(1), 26–57.
- Vrbik, I. and P. D. McNicholas (2014). Parsimonious skew mixture models for model-based clustering and classification. *Computational Statistics and Data Analysis* 71, 196–210.
- Wainwright, M. J., M. I. Jordan, et al. (2008). Graphical models, exponential families, and variational inference. *Foundations and Trends® in Machine Learning* 1(1–2), 1–305.
- Wang, Z., M. Gerstein, and M. Snyder (2009). RNA-Seq: a revolutionary tool for transcriptomics. *Nature Review Genetics* 10, 57–63.
- Wilkinson, L. and T. Gathani (2022, Feb). Understanding breast cancer as a global health concern. *The British Journal of Radiology*.

Wolfe, J. (1965, 05). A computer program for the maximum-likelihood analysis of types. pp. 57.